EurJOC
European Journal of Organic Chemistry

Research Article
doi.org/10.1002/ejoc.202500296

Chemistry Europe
European Chemical Societies Publishing

www.eurjoc.org

Unlocking Indazole Synthesis from α-Diazo-β-Ketoesters via Aryne Trapping: A Streamlined Approach

Souvik Guha, Aurélien Crochet, Thillaiarasi Sukumar, Mahesh Kumar Ravva, Subhabrata Sen, and Ludovic Gremaud*

Indazoles are high-value chemical building blocks used in medicinal chemistry and materials science for their distinct structural and functional features. This study details a [3 + 2]-cycloaddition reaction between various aryl-ketodiazoesters and *ortho*-(trimethylsilyl)aryl triflates under mild conditions, leading predominantly to 1-acyl-1*H*-indazoles. *N*-aryl-1*H*-indazoles and aryl benzoates are also observed as other products. The reaction exhibits broad functional group tolerance and scalability, making it a valuable synthetic approach. Mechanistic insights, derived from control experiments and density functional theory calculations, elucidate the cycloaddition pathway and rationalize the formation of the products. Collectively, these findings underscore the method's potential for synthesizing complex indazole derivatives, which hold significant promises for applications in pharmaceutical development and advanced materials research.

1. Introduction

Indazole and its derivatives exhibit wide range of biological and pharmaceutical properties.[1] Their favorable properties make them appealing targets for drug discovery.[2] Subsequently, the scaffold is integral to a variety of the Food and Drug Administration-approved drugs, thereby demonstrating its therapeutic versatility (**Figure 1**A). For instance, Granisetron-(**I**) is a 5-HT3 receptor antagonist utilized as an antiemetic to manage nausea and vomiting in chemotherapy patients.[3a] Indazole structures are also present among tyrosine kinase inhibitors such as Axitinib-(**VII**) and Entrectinib-(**II**), both effective in treating renal cell carcinoma.[3b,c] Other significant examples include Lonidamine-(**VI**), an antiglycolytic drug for brain tumor therapy,[3d] and SAM-531-(**IV**), also known as cerlapirdine, a potent 5-HT6 receptor antagonist evaluated in clinical trials for Alzheimer's disease.[3e] These drugs underscore the broad therapeutic applications of indazole derivatives in oncology, neurology, and several other therapeutic ailments. The multistep synthesis and functionalization of 1*H*-indazole structures present challenges in the efficient construction of specific target molecules, often impeding the swift development of synthetic pharmacophores.[4a–d] In general, arynes are promising intermediates in organic synthesis because of their reactivity, compatibility to react under mild reaction conditions and their ability to accommodate various functional groups. Recently, aryne-mediated methods have gained traction in pharmaceutical chemistry, for synthesizing indazole derivatives. A notable approach involves [3 + 2] cycloaddition of diazo compounds with arynes, which offers an appealing synthetic pathway to generate complex indazole frameworks. This method leverages the high reactivity of arynes, allowing for versatile modifications and enhanced yield efficiency in forming functionalized indazole derivatives, as illustrated in recent synthetic methodologies (Figure 1B,C). While the reaction between benzynes and diazo compounds was initially reported by Yamazaki et al.[5] (Figure 1B1) requiring significant heating to yield stable 1-acyl-1*H*-indazoles, our findings show notable differences from prior literature outcomes. Specifically, previous studies primarily generated 1*H*-indazoles or *N*-aryl-1*H*-indazoles when using diazoalkanes as substrates[6–8] (Figure 1C1). In ours, we demonstrate the formation of both 1-acyl and *N*-aryl-1*H*-indazoles, along with substantial formation of aryl benzoates, under mild reaction conditions (Figure 1D). Notably, reports on aryl benzoate formation via aryne pathways are limited, with only one other documented case involving aryl acid and aryl alcohol[9] (Figure 1C2).

Our [3 + 2] cycloaddition reaction, employing aryl-ketodiazoesters and arynes under mild conditions, demonstrates remarkable efficiency, achieving high yields of 1-acyl-1*H*-indazoles. This method shows excellent functional group tolerance, operates effectively at room temperature, and offers

S. Guha, L. Gremaud
HES-SO, HEIA-FR
University of Applied Sciences of Western Switzerland
Pérolles 80, CH-1700 Fribourg, Switzerland
E-mail: ludovic.gremaud@hefr.ch

A. Crochet
Department of Chemistry
University of Fribourg
Chemin du Musée 9, CH-1700 Fribourg, Switzerland

T. Sukumar, M. K. Ravva
Department of Chemistry
SRM University-AP
Amaravati, Andhra Pradesh 522240, India

S. Sen
Department of chemistry
School of Natural Sciences
Shiv Nadar Institution of Eminence Deemed to be University
Chithera, Uttar Pradesh 201314, India

Supporting information for this article is available on the WWW under https://doi.org/10.1002/ejoc.202500296

Research Article
doi.org/10.1002/ejoc.202500296

Chemistry Europe
European Chemical Societies Publishing

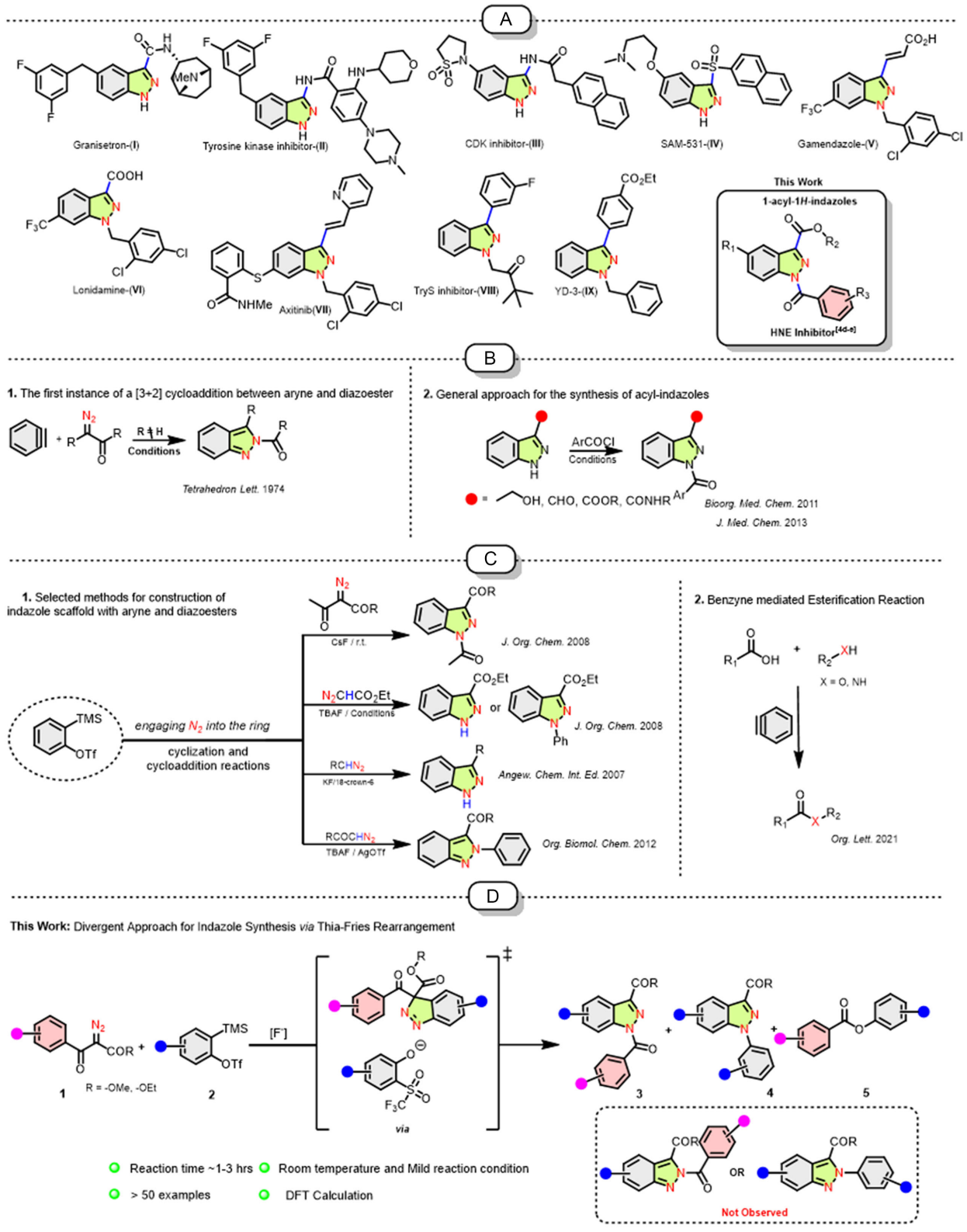

Figure 1. Overview of the work: A) Importance of biologically relevant Indazoles. B,C) Selected examples of [3 + 2] cycloaddition reaction between diazo and aryne and general approach for synthesis of 1-acyl-1*H*-indazoles. D) This work: divergent approach for indazole synthesis via thia-fries rearrangement.

significant scalability. Furthermore, the electronic nature of substituents on the aromatic ring of the ketodiazo compound influences product distribution. Electron-donating groups (EDGs) predominantly lead to the formation of 1-acyl-1*H*-indazoles, whereas electron-withdrawing groups (EWGs) favor the production of *N*-aryl-1*H*-indazoles and aryl benzoates. To further understand the observed product distribution, we conducted mechanistic studies and control experiments, which provide insights into the

Research Article
doi.org/10.1002/ejoc.202500296

formation pathways for each product and confirm the reaction's versatility and efficiency in producing various indazole derivatives.

2. Results and Discussion

Initially, ethyl 2-diazo-3-oxo-3-(*p*-tolyl)propanoate (**1aa**) and 2-(trimethylsilyl)phenyl trifluoromethanesulfonate (**2a**) were selected as model substrates to explore the aryne mediated [3 + 2]-cycloaddition reaction and to optimize the reaction conditions (**Table 1**). Building on previous findings,[6] we initiated a model reaction to further investigate in presence of CsF (0.5 eqiuv.) at room temperature for 10 h. The reaction progressed as anticipated, yielding the desired indazole product, ethyl 1-(4-methylbenzoyl)-1*H*-indazole-3-carboxylate (**3aa**), albeit in a modest 18% yield, with 80% of the unreacted starting material **1a** (entry 1, Table 1). Optimization efforts for this reaction included the addition of various additives, modifying the fluoride source and adjusting the stoichiometry of the aryne precursor (entries 2–7). Each of these led to a notable enhancement in yield, with a peak yield of 71% achieved at room temperature (entry 8) (see ESI.† for miscellaneous optimization). Control studies revealed that the reaction failed to proceed in the absence of CsF, underscoring its critical role. Interestingly, when CsF was replaced by KF, the yield of the product **3aa** dropped considerably under identical conditions, highlighting CsF as the preferred base for this transformation (entry 9). The reaction displayed good tolerance to polar aprotic solvents, such as THF and 2-methyl THF; however, the rate significantly decreased in these media, due to poor dissociation properties in tetrahydrofuran (entries 10–12). To gain a deeper understanding of the distribution of other minor products, it was observed that increasing the equivalent of the aryne precursor to 2.0–3.0 led to a significant decrease in the yield of **3aa**, dropping to 50%–40%. This suggests that higher concentrations of the aryne precursor may influence the reaction pathway, promoting side reactions or altering the selectivity (entries 13–15). This effect suggests that higher aryne equivalents may favor competing pathways, specifically enhancing *N*-aryl-1*H*-indazole formation. Furthermore, acetonitrile (ACN) was found to be essential for this transformation, while reaction temperature had no significant influence on yield or product distribution, confirming the stability of the optimized conditions.

3. Scope and Limitations

With the optimized conditions for the indazole formation of in hand (entry 8, Table 1), we explored the scope of the aryne-mediated cycloaddition reactions. A range of (aryl)-ketodiazo substrates (**1**) were evaluated with substituted aryne (**2a** or **2b**),

Table 1. Optimization of the reaction conditions.[a)]

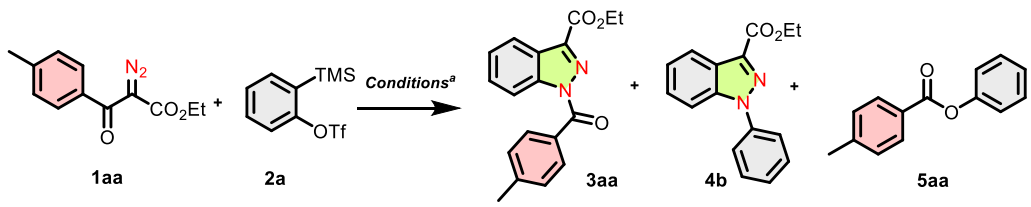

1aa 2a 3aa 4b 5aa

Entry	2a equiv.	[F⁻] equiv.	Additive equiv.	Solvent	Time	%Yield[b)] 3aa	%Yield[b)] [overall] 4b + 5aa
1	0.5	CsF (1.0)	None	CH_3CN	10 h	18%	≈5.0%
2	0.5	CsF (1.0)	$CsCO_3$ (0.5)	CH_3CN	10 h	21%	≈5.0%
3	1.0	CsF (1.0)	$CsCO_3$ (0.5)	CH_3CN	10 h	38%	10%
4	1.0	KF (1.0)	18-c-6 (0.5)	CH_3CN	5 h	36%	10%
5	1.5	CsF (1.0)	18-c-6 (0.5)	CH_3CN	5 h	49%	15%
6	1.5	CsF (1.2)	18-c-6 (0.5)	CH_3CN	5 h	62%	21%
7	1.5	CsF (1.2)	18-c-6 (1.0)	CH_3CN	5 h	70%	23%
8	**1.5**	**CsF (1.2)**	**18-c-6 (1.0)**	**CH_3CN**	**1 h**	**71%**	**23%**
9	1.5	KF (1.2)	18-c-6 (1.0)	CH_3CN	1 h	40%	16%
10	1.5	CsF (1.2)	18-c-6 (1.0)	THF	5 h	44%	12%
11	1.5	CsF (1.2)	18-c-6 (1.0)	THF	10 h	70%	22%
12	1.5	KF (1.2)	18-c-6 (1.0)	2Me-THF	10 h	69%	19%
13	2.5	CsF (1.2)	18-c-6 (1.0)	CH_3CN	2 h	56%	28%
14	3.0	CsF (1.2)	18-c-6 (1.0)	CH_3CN	2 h	50%	38%
15	3.0	CsF (1.2)	18-c-6 (1.0)	CH_3CN	3 h	46%	43%

[a)]Unless otherwise noted, reactions were conducted using **1aa** (0.43 mmol) using 3 mL solvent at room temperature. [b)]Isolated yield. Abbreviations: 18-c-6 = 18-crown-6, THF = tetrahydrofuran, 2Me-THF = 2-methyltetrahydrofuran.

as illustrated in **Scheme 1**, to obtain the compound **3**. Owing to the air stability of aryl-ketodiazoesters (**1**), all separation steps were performed under open air conditions. Nonsubstituted aryl-ketodiazoesters (**3af**)[10] and EDGs such as naphthyl (**3ad**, **3bd**), 4-^{t}Bu (**3ab**, **3bb**), 4-Me (**3aa**, **3ba**), and 4-Et (**3ae**, **3be**) were highly compatible, resulting in good yields around 70%–80%. Halogen substituents at the paraposition, such as 4-Cl (**3aj**, **3bg**) and 4-Br (**3ai**, **3bf**), produced moderate yields, while ortho- and metasubstituted EDGs like methyl (**3bi**, **3bk**) yielded slightly lower than their parasubstituted counterparts. In contrast, ortho- and metahalogenated -Br/-Cl groups (**3al**, **3bj**, and **3bm**) did not exhibit significant yield differences from the substituted versions. For substrates bearing EWGs such as -CN, -F, and -CF_3 on the benzene ring, it was essential to modify the reaction conditions to ensure optimal reactivity and yield. Specifically, in these cases, the aryl-ketodiazo compounds were dissolved in ACN and introduced to the ortho-(trimethylsilyl)aryl triflates (**2**) solution through a dropwise addition over a 15-min period. This controlled addition helped regulate the reactivity of the diazo compounds with the activated benzene ring, leading to improved yields. Notably, the positional variation of these EWGs on the aromatic ring, whether at the para, meta, or ortho positions, did not significantly affect the product yield, suggesting a high tolerance to substitution pattern in these reactions. Moreover, any alteration in the R group, specifically substituting CO_2Me or CO_2Et, also did not markedly impact the overall yield. When investigating the reactivity of

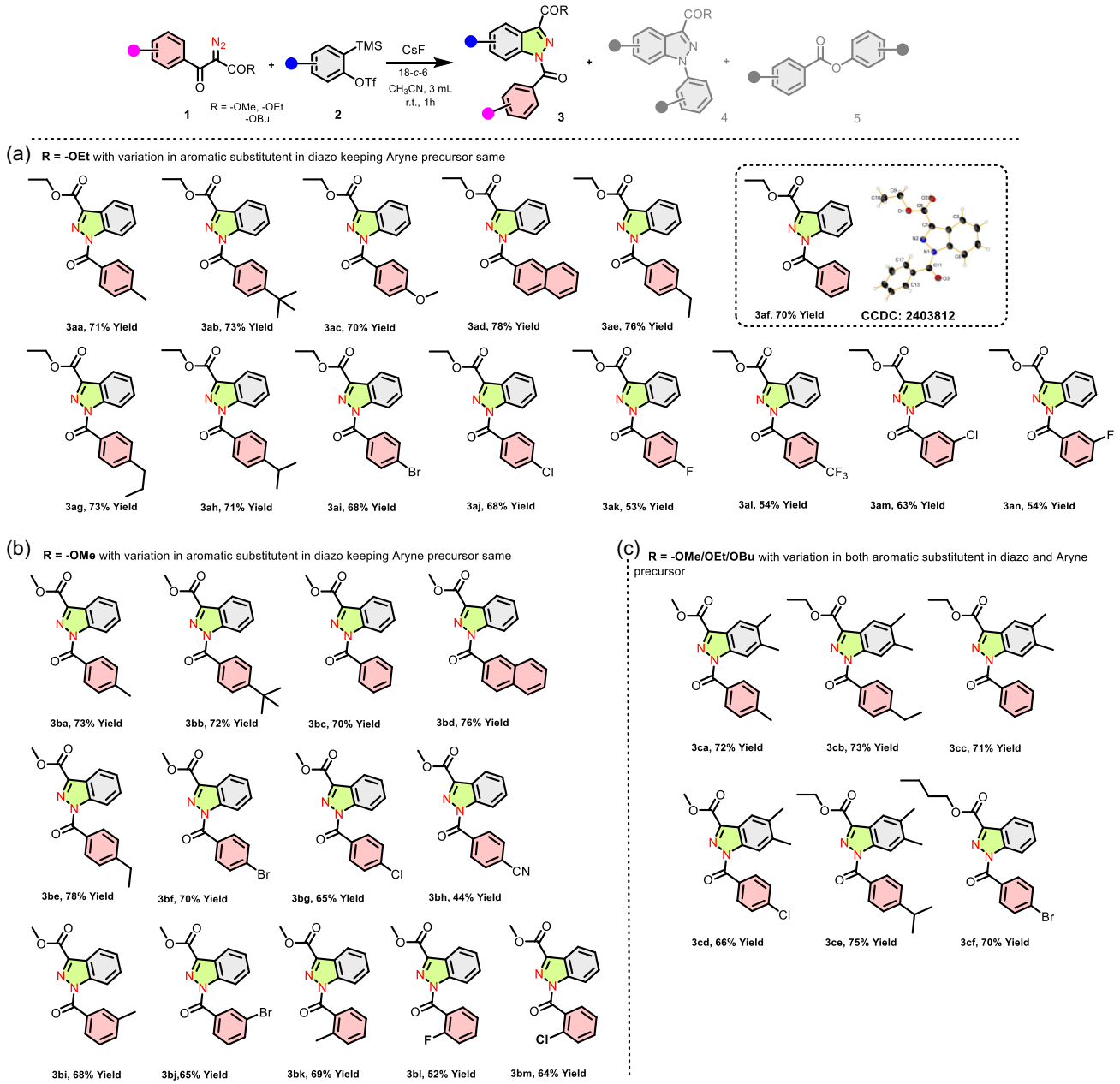

Scheme 1. Substrate scope of 1-acyl-1*H*-indazoles. Unless until mentioned, all the reactions were conducted using 1 (1.0 equiv.), 2 (1.5 equiv.), CsF (1.2 equiv.), 18-crown-6 (1.0 equiv.), and CH_3CN (3.0 mL) at room temperature for 1 h. The yields are calculated based on the isolated quantities of the product.

Research Article
doi.org/10.1002/ejoc.202500296

ortho-(trimethylsilyl)aryl triflates (**2**) substituted with 4,5-dimethyl groups (**2b**) in combination with parasubstituted derivatives (Cl, Me, Pr, or Et) to yield compounds such as **3ca**, **3cb**, **3cd**, and **3ce**, the reactions proceeded efficiently. The isolated yields of these derivatives were comparable to those obtained with unsubstituted ortho-(trimethylsilyl)aryl triflates (**2a**), indicating that the 4,5-dimethyl substitution had minimal impact on the overall reaction efficiency. This similarity in reactivity suggests that the presence of substituents on the phenyl ring, including steric or electronic variations, does not significantly influence the formation of the indazole product except when nitrosubstituted substrate is used. Indeed, 4-nitro-substituted α-diazo-β-ketoester, underwent complete conversion into the corresponding compounds **4** and **5** within a very short reaction time. This outcome can be attributed to the strong electron-withdrawing nature of the nitro group, which significantly stabilizes the transition state in Step 3 of the reaction mechanism, as supported by our computational studies. The energetic preference for this pathway explains the exclusive formation of byproducts rather than the desired 1-acyl-1*H*-indazole. The same trend and conclusion were observed with the *N*,*N*-dimethylamino-substituted α-diazo-β-ketoester. The investigation of minor product formation was conducted as outlined in (entry 15, Table 1), with the evaluation of reactions using substituted arynes (**2a** and **2b**), as demonstrated in **Scheme 2**. Notably, the formation of *N*-aryl-1*H*-indazoles (**4a–4d**)[11] proceeded with yields around 23%–27%, indicating a reliable synthesis for these derivatives. In contrast, the formation of benzoate derivatives displayed greater variability, with a yield range spanning from 18% to 30%. This variation in benzoate yield reflects a broad tolerance for benzoate formation across different aryne substrates, showcasing the versatility of this reaction in accommodating a range of substituents while yielding indazoles and benzoate products efficiently.

4. Mechanistic Investigation and Application

To elucidate the underlying reaction mechanism, a series of experiments were performed. Initially, the addition of 2.0 equivalents of radical scavengers (BHT and 1,1-diphenylethylene) to

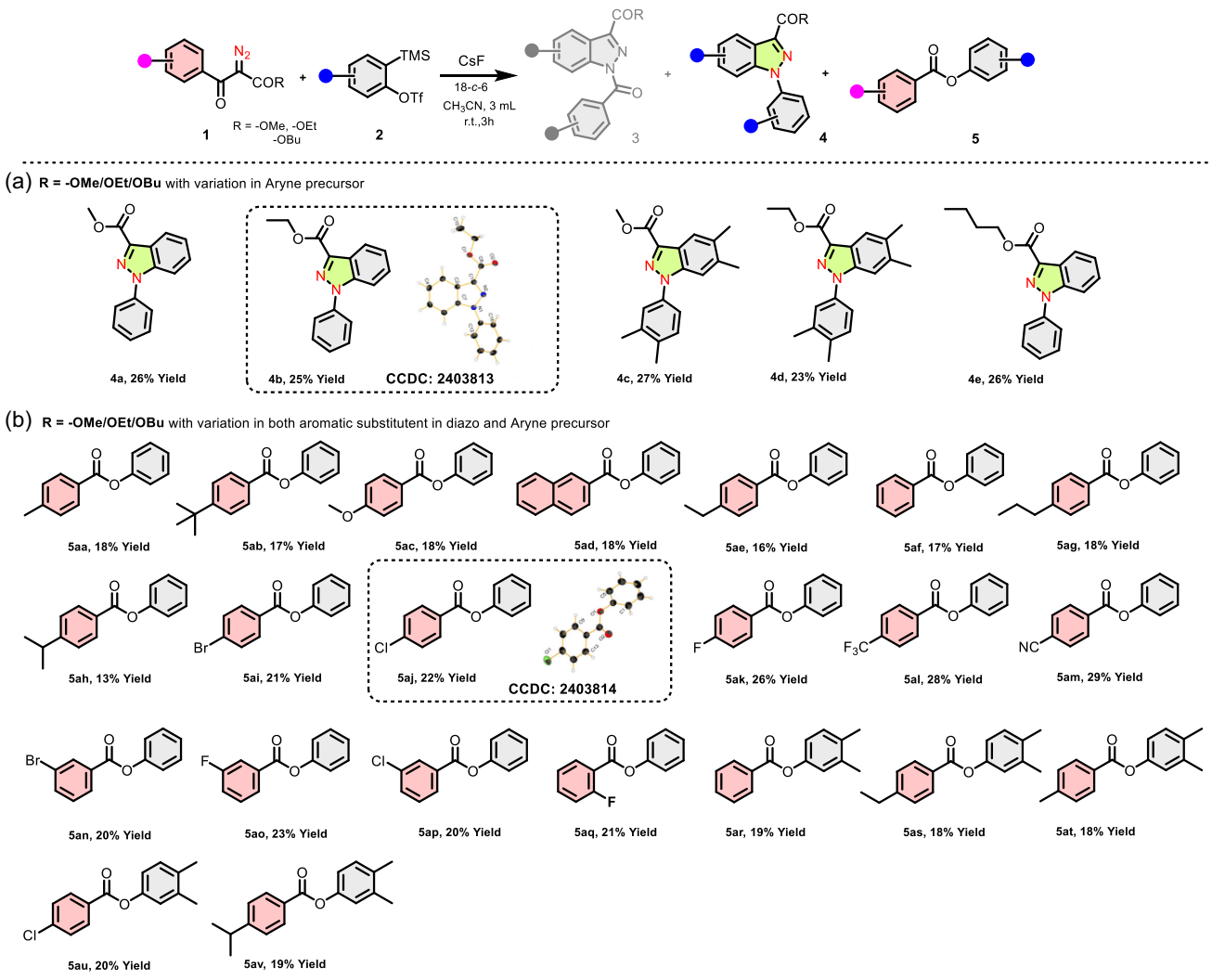

Scheme 2. Substrate scope of *N*-aryl-1*H*-indazoles and aryl benzoates. Unless until mentioned, all the reactions were conducted using 1 (1.0 equiv.), 2 (3.0 equiv.), CsF (1.5 equiv.), 18-crown-6 (1.0 equiv.), and CH_3CN (3.0 mL) at room temperature for 3 h. Yields based on isolated amount.

Research Article
doi.org/10.1002/ejoc.202500296

the reaction system separately demonstrated no significant impact on reaction progression (**Scheme 3**a), suggesting that radical pathways are not a dominant mechanism here. We hypothesize, based on extensive literature reports,[6–8] that the 1-acyl-1*H*-indazoles (**3**) structure arises predominantly from a [3 + 2]-cycloaddition reaction between the (aryl)-ketodiazo (**1**) precursor and aryne (**2**) intermediates. However, to gain further insight into the formation pathways of *N*-aryl-1*H*-indazoles (**4**) and aryl benzoates (**5**) derivatives,[12] additional experiments were designed to probe possible intermediates and mechanistic steps. To explore these pathways, 3-(trimethylsilyl)naphthalen-2-yl tri-fluoromethanesulfonate (**2c**) was subjected to the optimized reaction conditions (Table 1, entry 8) at ambient temperature, resulting in the isolation of the aryne trapping product, 2-(naphthalen-2-yloxy)-3-((trifluoromethyl)sulfonyl)naphthalene (**8**) (triflone),[13] in a yield of 54% yield within 60 min (Scheme 3b). This rapid trapping is consistent with a thia-fries rearrangement mechanism,[14] strongly supporting the involvement of 3-((trifluoromethyl)sulfonyl)naphthalen-2-olate intermediates (**A**). In a parallel experiment, aryl-ketodiazo (**1aj**) and **2b** were reacted according to (Table 1, entry 8) and analyzed by ESI-MS (m/z: 205.4) (see ESI.†). These analyses confirmed the formation of methyl 5,6-dimethyl-1*H*-indazole-3-carboxylate (**B**) (Scheme 3c), suggesting that aryne trapping by 5,6-dimethyl-1*H*-indazole may serve as a mechanistic pathway for the generation of *N*-aryl-1*H*-indazole (**4**). Collectively, these control experiments robustly indicate the involvement of a thia-fries rearrangement in facilitating aryne trapping, shedding light on the reaction mechanism and the selective formation of these indazole derivatives. To investigate the substituent effects of the aryl-ketodiazo substrates (**1**) and the aryne intermediate (**2**) on intermediate formation and the yield of the final product equimolar quantities of each reactant (**1aa**, **1al**) were reacted under standard conditions for 1 h, after which the pure products were isolated via flash column chromatography. The electron-donating 4Me-analogue **3aa** was produced in a 3:1 ratio over the 4CF_3-substituted **3ka**, achieving an overall yield of 60% (Scheme 3d).

Next, the reaction was successfully scaled up to a 0.0033 mol, producing ethyl 1-(4-bromobenzoyl)-1*H*-indazole-3-carboxylate (**3ai**) with an impressive, isolated yield of 69% (Scheme 3e), underscoring the robustness and scalability of this methodology for generating target compounds in larger quantities. This high yield facilitates further synthetic manipulation and derivatization with minimal material loss. To demonstrate the versatility of the indazole derivative (**3ai**) as a synthetic intermediate, we explored subsequent transformations (Scheme 3f). Under basic conditions, (**3ai**) underwent a Suzuki cross-coupling reaction[15] with phenylboronic acid (**6**), yielding the corresponding ethyl 1-([1,1′-biphenyl]-4-carbonyl)-1*H*-indazole-3-carboxylate (**7**) in 21%, showcasing the feasibility of palladium-catalyzed coupling in expanding molecular complexity. This efficient conversion highlights the accessibility of indazole derivatives from **3ai**, broadening the scope of functionalization pathways available for further application and structural diversification.

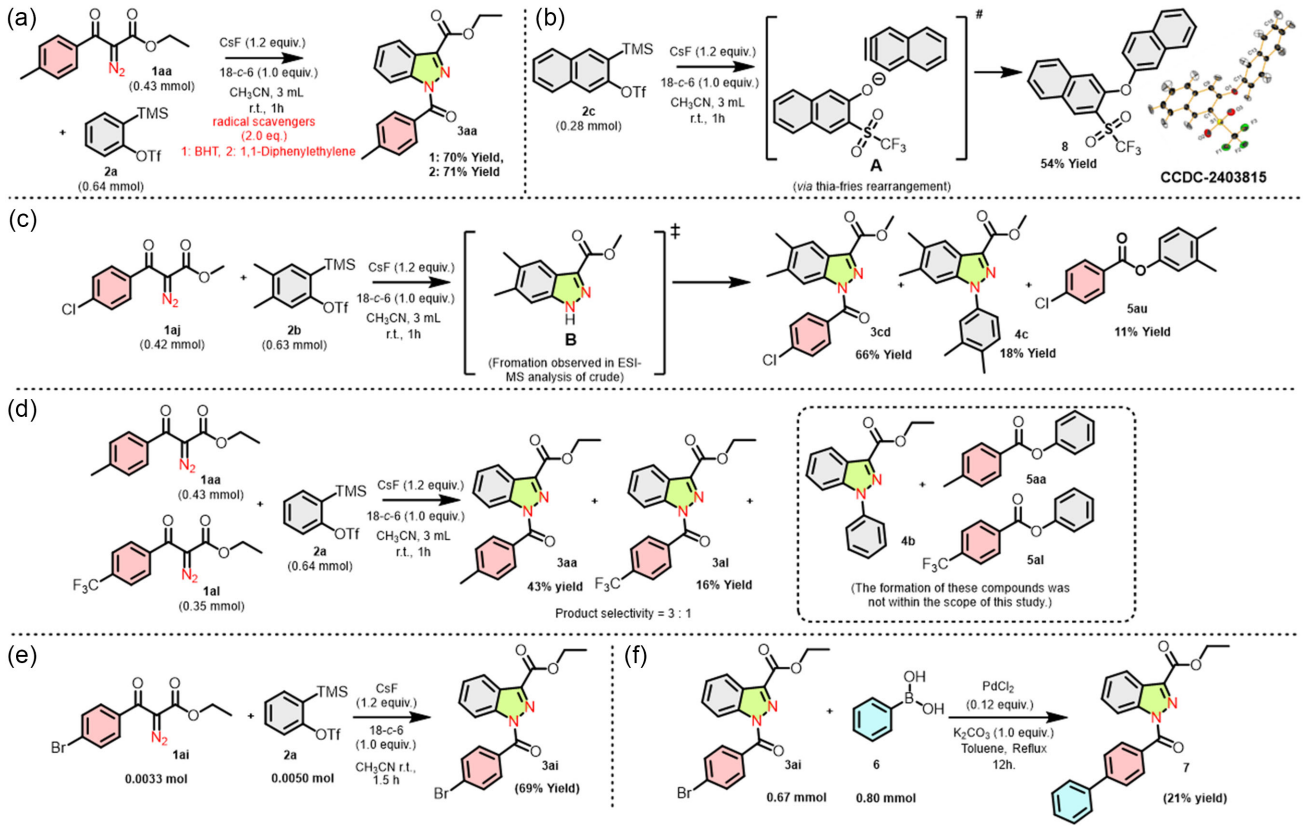

Scheme 3. Mechanistic investigation and application. a) A radical-trapping experiment, b) a room-temperature thia-fries rearrangement, c) studies on the formation of a 1*H*-indazole intermediate, d) a crossover experiment, e) gram scale synthesis, and f) postsynthetic transformation.

Research Article
doi.org/10.1002/ejoc.202500296

Chemistry Europe
European Chemical Societies Publishing

5. Proposed Mechanism and DFT Calculations

For a deeper understanding of the reaction mechanism, we have depicted the mechanism and showcased the density functional theory (DFT) calculations that were employed, as illustrated in **Figure 2**d. The molecular geometries of all structures—reactants, intermediates, transition states, and products—were optimized using the B3LYP functional and the 6–31 G(d,p) basis set[16–18]

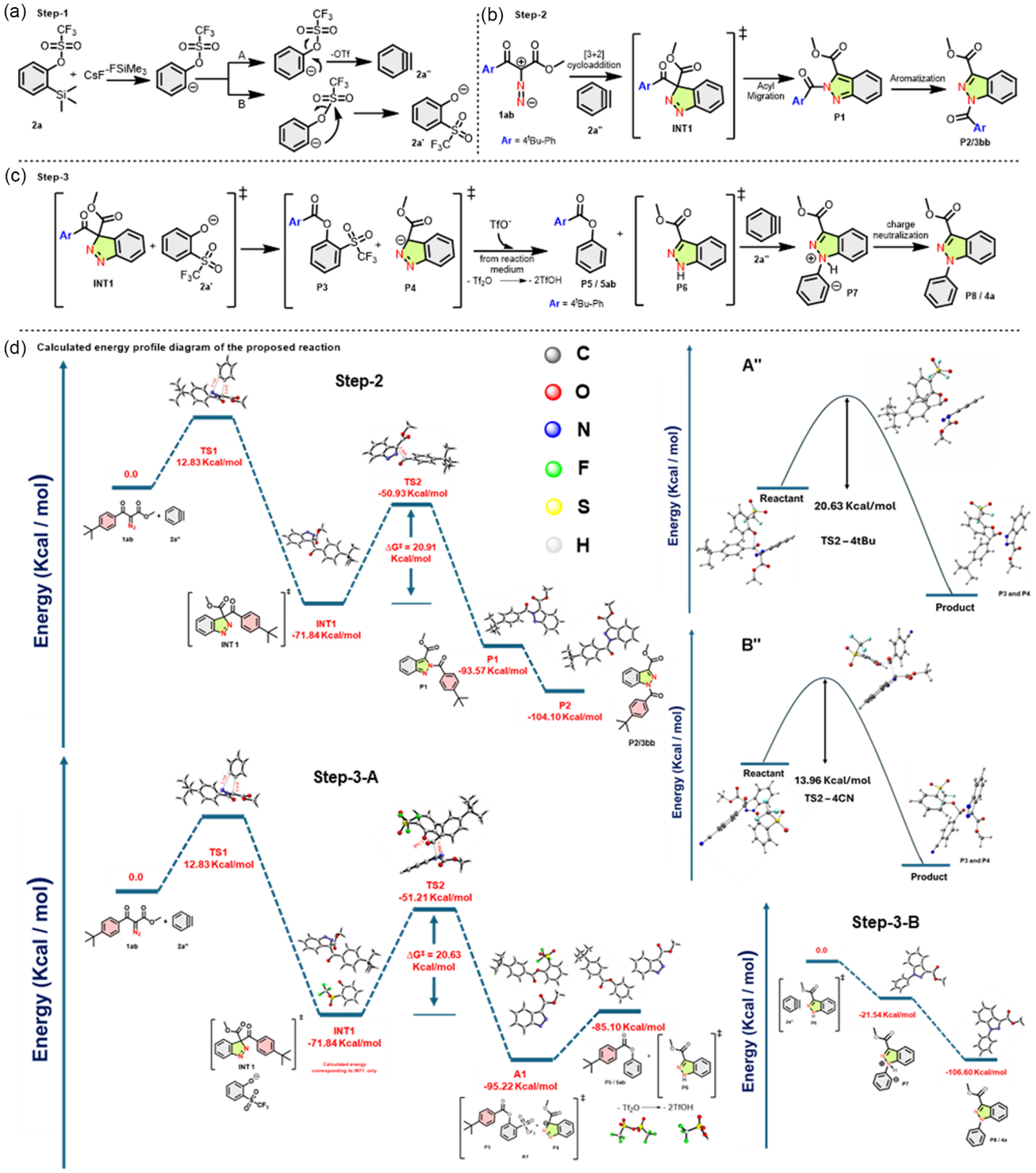

Figure 2. Proposed mechanism and DFT analysis. a) Suggested pathway for benzyne formation, and the generation of thia-Fries rearranged intermediates. b) [3 + 2] Cycloaddition mechanism between the diazo compound and aryne for the synthesis of 1-acyl-1*H*-indazoles. c) Probable reaction pathway for the formation of *N*-aryl-1*H*-indazoles and arylbenzoates. d) Calculated energy profile diagram of the proposed reaction pathway, as determined by B3LYP/6-31 G(d,p) computational methods. Optimized geometries of all species involved—reactants, transition states, intermediates, and products. Step 2: Reaction path for 3bb. Step 3: A/3B-Reaction path for 5ab/4b. A"/B" represents critical transition state for P3/P4 formation.

with no symmetry constraints applied. Calculations were conducted using the Gaussian 16 software package.[19]

In Figure 2a, the mechanism begins with fluoride treatment of **2a**, leading to C—Si bond cleavage and subsequent formation of benzyne (**2a″**) and a thia-fries rearranged intermediate (**2a′**). This rearrangement results from the anionic intermediate generated in the initial step. Moving to Figure 2b, diazo compounds containing acyl groups on the diazo carbon (**1ab**) first undergo a [3 + 2] cycloaddition with benzyne (**2a″**), forming 3,3-disubstituted 3*H*-indazole intermediates (**INT1**). Through acyl migration, **INT1** is converted into 1-acyl-1*H*-indazoles (**3ab**), as shown in the free energy profile of Figure 2d. In this energy diagram, the Gibbs free energy (**ΔG**) of the starting materials (**1ab** and **2a**) is set as the baseline. Calculations indicate that the formation of the initial transition state (**TS1**) requires an energy input of ≈12.83 kcal mol^{-1}. The cycloaddition between **1ab** and **2a** results in the intermediate **INT1**, via **TS1** characterized by N—C and C—C bond lengths of 2.72 and 2.41 Å, respectively. Acyl migration from C3 to N2 in **INT1** occurs via **TS2** with an energy barrier of 20.91 kcal mol^{-1} and a C—C bond length of 2.08 Å, yielding an unstable, non-aromatic intermediate (**P1**). This intermediate subsequently rearranges to form the more stable 1-acyl-1*H*-indazole (**3ab**/**P2**) by migration to N1. In Figure 2c, pathways for *N*-aryl-1*H*-indazole (**4a**) and arylbenzoates (**5ab**) formation are explored in "**Step-3A**" and "**Step-B**." In **Step-3 A**, the interaction of **INT1** with **2a**′ produces intermediates **P3** and **P4** with an energy barrier of 20.63 kcal mol^{-1} and a C—C bond length of 1.99 and 1.74 Å. This step is considered a critical transition state for determining product distribution and selectivity among different EDGs and EWGs. Computational screening of this step was conducted with representative EDGs like 4-^{t}Bu and EWGs such as 4-CN. The results reveal that in **Step-3A**, the **4-CN** functionality exhibits a lower energy barrier of 13.96 kcal mol^{-1} for the formation of intermediates **P3**/**P4**, whereas the 4-^{t}Bu substituent requires a significantly higher energy barrier of 20.63 kcal mol^{-1} for the same step. These findings suggest that EWG-substituted systems are more favorable for overcoming the energy barrier compared to EDG-substituted systems, thereby influencing the overall reactivity and product selectivity in the reaction pathway. Initially, we hypothesized that the formation of **P5** and **P6** involved hydrolysis facilitated by dissolved water or moisture, given the known moisture-absorbing properties of crown ethers

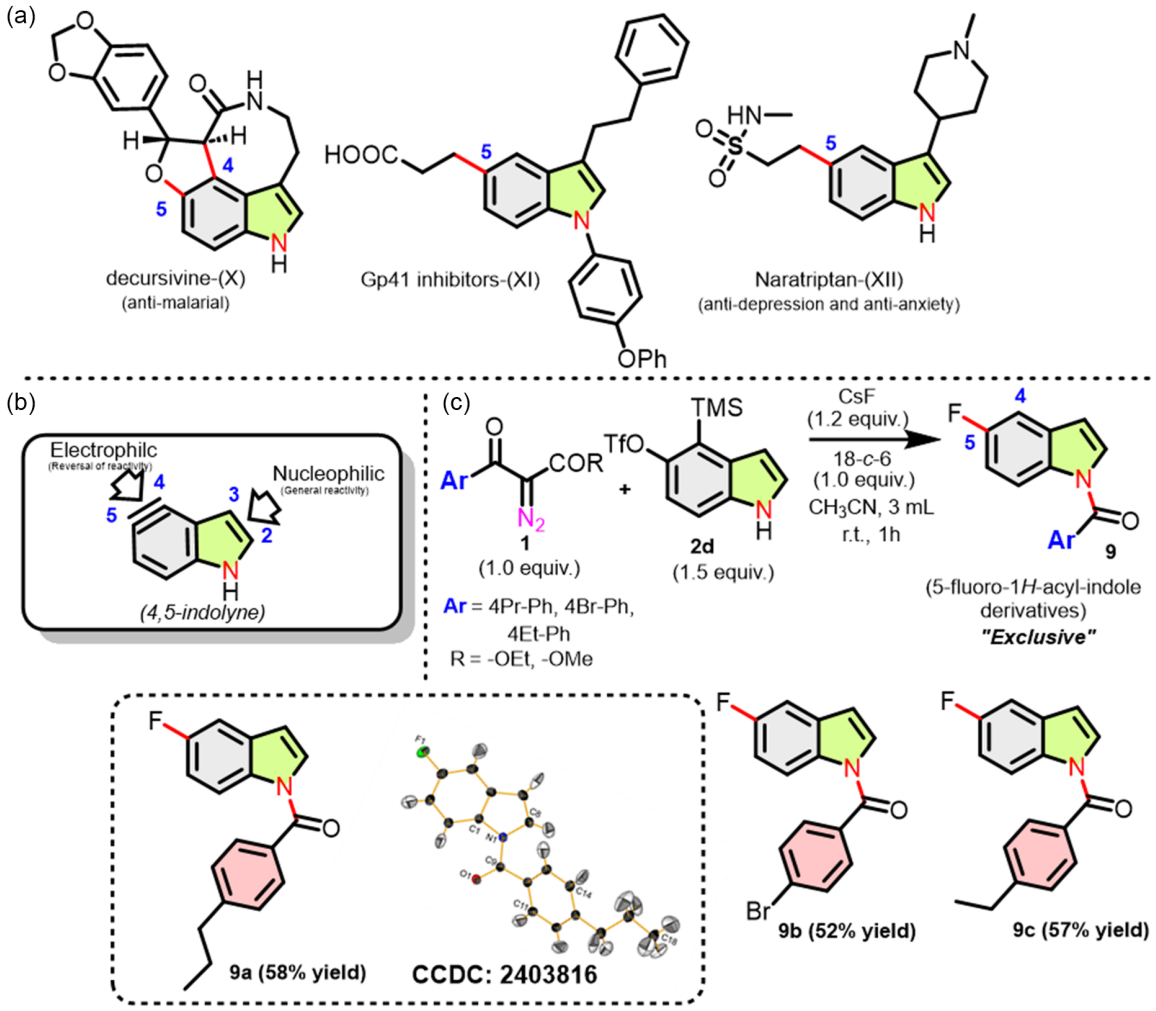

Figure 3. Diversity. a) Pharmaceutically relevant indole motifs, b) reversal of reactivity in indoles, and c) reaction with Garg 4,5-indolyne precursor with aryl-ketodiazo under standard condition.

(due to their oxygen rich structures, which facilitate hydrogen bonding with water molecules) and the fact that the reaction was conducted under open-air conditions. However, Karl Fischer analysis revealed that the trace amounts of water present were insufficient to hydrolyze the specific molar quantities required for **P5** and **P6** formation. This finding suggests that triflic acid likely plays a catalytic role in the formation of **P5** and **P6**, rather than moisture-induced hydrolysis (see ESI.†). Next the excess aryne (**2a″**) in the system interacts with **P6**, resulting in the formation of **P7** which undergoes to charge neutralization process to generate *N*-aryl-1*H*-indazole (**4a**/**P8**).

6. Reaction with Garg 4,5-Indolyne Precursor

The indole heterocycle is an essential framework (**Figure 3**a) found in a vast array of bioactive natural products and medicinal agents, with compounds like Decrusivine-(**X**), Gp-41 inhibitors-(**XI**), and Naratriptan-(**XII**) serving as notable examples.[20–22] To explore indole-based transformations, we selected 4,5-indolyne (Figure 3b) as a primary substrate and reacted it with various aryl-ketodiazo compounds, aiming to synthesize a fused indole-indazole structure. Unexpectedly, despite following the optimized reaction conditions (Table 1, entry 8), the reaction yielded an exclusive 4-fluoro-substituted-1-acyl-1*H*-indole derivative (**9a-9c**),[23] accompanied by a complex mixture of uncharacterized byproducts as identified through NMR analysis (Figure 3c). The formation of this fluorinated product likely results from CsF-mediated fluorination within the reaction. Additionally, the NH-free indolyne precursor may have contributed to the initial destabilization of the aryl-ketodiazo intermediate, potentially altering the pathway and yielding complex side products. Interestingly, selective fluorination at the 5-position in 4,5-indolyne systems is generally expected, as prior research indicates that nucleophilic substitution at this site is typically favored due to both electronic and steric factors.[24] However, in this case, the observed reactivity may stem from multiple contributing factors. These could include the direct displacement of the -OSO_2CF_3 group by fluoride, which may proceed through a pathway involving minimal steric hindrance and enhanced nucleophilicity of fluoride ions. This type of fluorination process, however, is not generally observed in aryne reactions, where different substitution patterns typically dominate. Given these findings, we are initiating further studies to thoroughly investigate the reactivity of 4,5-indolyne derivatives under varied conditions in our upcoming project.

7. Conclusions

In summary, we have developed an aryl-ketodiazo-mediated [3 + 2] cycloaddition reaction with arynes, enabling the efficient synthesis of indazoles with high regioselectivity and broad substrate compatibility. Diazo compounds featuring carbonyl groups attached to the diazo carbon undergo acyl migration to yield 1-acyl-1*H*-indazoles, while using an excess of aryne precursor facilitates the formation of *N*-aryl-1*H*-indazoles. This approach allows for the streamlined synthesis of arylbenzoates from readily available materials. Initial mechanistic studies indicate key reaction pathways, offering insights into the formation process. This methodology presents a valuable strategy for constructing indazole derivatives with potential biological and pharmaceutical applications. Ongoing research aims to further explore the synthesis and functional applications of 4,5-indolyne precursors.

8. Experimental Section

General Procedure for Preparation of α-Diazo-β-Keto Esters (1aa-1ca)

According to prior literature,[25] the preparation of acetoacetate derivatives was carried out as follows: A dried 100 mL three-necked flask was charged with NaH (2.2 g, 60% w/w, 56 mmol), dimethyl carbonate, diethyl carbonate, di-n-butyl carbonate (40 mmol), and toluene (20 mL) under a nitrogen atmosphere. The reaction mixture was heated to reflux in an oil bath, and a solution of acetophenone (20 mmol) in toluene (10 mL) was added dropwise for over 30 min. After hydrogen evolution ceased (30–45 min), the mixture was cooled to room temperature. Glacial acetic acid (6 mL) was then added dropwise, resulting in the formation of a heavy pasty solid. Icecold water was added gradually until the solid dissolved completely. The mixture was diluted with ethyl acetate (EtOAc), and the organic layer was separated, washed sequentially with water (20 mL) and saturated brine (20 mL) and dried over anhydrous Na_2SO_4. The solvent was removed under reduced pressure, and the residue was used directly for the subsequent step. For the next step, following previous literature,[26] α-diazoesters were synthesized: To a cooled solution of acetoacetate derivatives (1.0 equiv, 5 mmol) and *p*-acetamidobenzenesulfonyl azide (p-ABSA) (1.2 equiv, 6 mmol) in anhydrous CH_3CN at 0 °C, triethylamine (Et_3N) (3.0 equiv, 15 mmol) was added dropwise. The reaction mixture was stirred at room temperature for 5 h and then concentrated in vacuo. Water (20 mL) was added, and the mixture was extracted with diethyl ether (2 × 20 mL). The combined organic extracts were washed with brine (20 mL), dried over Na_2SO_4, and the solvent was removed under reduced pressure. The resulting residue was purified via flash column chromatography using heptane/ethyl acetate as the eluent, yielding the desired diazo compounds **1.**

General Procedure for Preparation of 1-acyl-1H-Indazole (A)

In a 10 mL screw-cap vial equipped with a magnetic stir bar, compound **1** (1.0 equiv.) and compound **2** (1.5 equiv.) were introduced under ambient air conditions. CsF (1.2 equiv.), 18-crown-6 (1.0 equiv.), and CH_3CN (3.0 mL, 99.90% extra dry) were subsequently added at room temperature, and the mixture was stirred for 1 h. The reaction progress was monitored by thin-layer chromatography (TLC). Upon complete consumption of compound **1**, the solvent was removed under reduced pressure. The residue was then diluted with EtOAc, and the organic layer was separated, washed sequentially with water (5 mL) and saturated brine (5 mL), and then dried over anhydrous Na_2SO_4. The product was purified by column chromatography on silica gel (SiO_2) using a hexane/EtOAc gradient (95:5 to 90:10, $R_f = 0.2$)] to afford **3**.

General Procedure for Preparation of N-aryl-1H-Indazole and Arylbenzoates (B)

In a 10 mL screw-cap vial equipped with a magnetic stir bar, compound **1** (1.0 equiv.) and compound **2** (3.0 equiv.) were introduced under ambient air conditions. CsF (1.5 equiv.), 18-crown-6 (1.0 equiv.), and CH_3CN (3.0 mL, 99.90% extra dry) were subsequently added at

room temperature, and the mixture was stirred for 3 h. The reaction progress was monitored by thin-layer chromatography. Upon complete consumption of compound **1**, the solvent was removed under reduced pressure. The residue was then diluted with EtOAc, and the organic layer was separated, washed sequentially with water (5 mL) and saturated brine (5 mL), and then dried over anhydrous Na_2SO_4. The product was purified by column chromatography on silica gel (SiO_2) using a hexane/EtOAc gradient (95:5 to 90:10, $R_f = 0.2$)] to afford **4** and **5**.

Supporting Information

The authors have cited additional references within the Supporting Information.

Acknowledgements

The authors would like to thank the State Secretariat for Education, Research and Innovation (SERI) of the Swiss Confederation to have received a research grant commissioned by ZHAW: "Leading House South Asia and Iran, Zurich University of Applied Sciences". L.G. would like to thank the Chemistry Department, as well as the ChemTech Institute, of University of Applied Sciences Western Switzerland, Faculty of Engineering and Architecture, for the technical, operational, as well as the financial support. S.S. is thankful to Shiv Nadar Institution of Eminence, deemed to be University for funding and facility.

Conflict of Interest

The authors declare no conflict of interest.

Data Availability Statement

The data that support the findings of this study are available in the supplementary material of this article.

Keywords: [3 + 2] Cycloaddition · density functional theory · indazoles · mechanistic insights · scalable synthesis

[1] a) A. Thangadurai, M. Minu, S. Wakode, S. Agrawal, A. Narasimhan, *Med. Chem. Res.* **2012**, *21*, 1509; b) D. D. Gaikwad, A. D. Chapolikar, C. G. Devkate, K. D. Warad, A. P. Taya-de, R. P. Pawar, A. J. Domb, *Eur. J. Med. Chem.* **2015**, *90*, 707; c) J. Dong, Q. Zhang, Z. Wang, G. Huang, S. Li, *ChemMedChem* **2018**, *13*, 1490; d) S. G. Zhang, C. G. Liang, W. H. Zhang, *Molecules* **2018**, *23*, 2783.
[2] A. Jennings, M. Tennant, *J. Chem. Inf. Model.* **2007**, *47*, 1829.
[3] a) R. Navari, D. Grandara, P. Hesketh, S. Hall, J. Mailliard, H. R. Friedman, D. Fitts, *J. Clin. Oncol.* **1995**, *13*, 1242; b) V. Grünwald, A. S. Merseburger, *OncoTargets Ther.* **2012**, *5*, 111; c) S. J. Modi, V. M. Kulkarni, *Med. Drug Discovery* **2019**, *2*, 100009; d) K. Nath, L. Guo, B. Nancolas, D. S. Nelson, A. A. Shestov, S. C. Lee, J. Roman, R. Zhou, D. B. Leeper, A. P. Halestrap, I. A. Blair, J. D. Glickson, *Bio-chim. Biophys. Acta, Rev. Cancer.* **2016**, *1866*, 151; e) C. Y. Cheng, B. Silvestrini, J. Grima, M. Mo, L. Zhu, E. Johansson, L. Saso, M. G. Leone, M. Palmery, D. Mruk, *Biol. Reprod.* **2001**, *65*, 449.
[4] a) H. Ferrero, M. Solas, P. T. Francis, M. J. Ramirez, *CNS Drugs.* **2017**, *31*, 19; b) Z. Liu, L. Wang, H. Tan, S. Zhou, T. Fu, Y. Xia, Y. Zhang, J. Wang, *Chem. Commun.* **2014**, *50*, 5061; c) L. Zhang, J. Chen, X. Chen, X. Zheng, J. Zhou, T. Zhong, Z. Chen, Y. F. Yang, X. Jiang, Y. B. She, C. Yu, *Chem. Commun.* **2020**, *56*, 7415; d) L. Crocetti, I. A. Schepetkin, A. Cilibrizzi, A. Graziano, C. Vergelli, D. Giomi, A. I. Khlebnikov, M. T. Quinn, M. P. Giovannoni, *J. Med. Chem.* **2013**, *56*, 6259; e) L. Crocetti, M. P. Giovannoni, I. A. Schepetkin, M. T. Quinn, A. I. Khlebnikov, A. Cilibrizzi, V. Dal Piaz, A. Graziano, C. Vergelli, *Bioorg. Med. Chem.* **2011**, *19*, 4460.
[5] T. Yamazaki, G. Baum, H. Shechter, *Tetrahedron Lett.* **1974**, *15*, 4421.
[6] Z. Liu, F. Shi, P. D. Martinez, C. Raminelli, R. C. Larock, *J. Org. Chem.* **2008**, *73*, 219.
[7] T. Jin, Y. Yamamoto, *Angew. Chem. Int. Ed.* **2007**, *46*, 3323.
[8] C. D. Wang, R. S. Liu, *Org. Biomol. Chem.* **2012**, *10*, 8948.
[9] J. Zhao, J. Shi, Y. Li, *Org. Lett.* **2021**, *23*, 7274.
[10] Deposition Number(s) 2403812 (for 3af), contain(s) the supplementary crystallographic data for this paper. These data are provided free of charge by the joint Cambridge Crystallographic Data Centre and Fachinformationszentrum Karlsruhe Access Structures service.
[11] Deposition Number(s) 2403813 (for 4b) contain(s) the supplementary crystallographic data for this paper. These data are provided free of charge by the joint Cambridge Crystallographic Data Centre and Fachinformationszentrum Karlsruhe Access Structures service.
[12] Deposition Number(s) 2403814 (for 5aj) contain(s) the supplementary crystallographic data for this paper. These data are provided free of charge by the joint Cambridge Crystallographic Data Centre and Fachinformationszentrum Karlsruhe Access Structures service.
[13] Deposition Number(s) 2403815 (for 8) contain(s) the supplementary crystallographic data for this paper. These data are provided free of charge by the joint Cambridge Crystallographic Data Centre and Fachinformationszentrum Karlsruhe Access Structures service.
[14] Y. Himeshima, T. Sonoda, H. Kobayashi, *Chem. Lett.* **1983**, *12*, 1211.
[15] S. Li, Y. Lin, J. Cao, S. Zhang, *J. Org. Chem.* **2007**, *72*, 4067.
[16] C. Lee, W. Yang, R. G. Parr, *Phys. Rev. B* **1988**, *37*, 785.
[17] A. D. Becke, *J. Chem. Phys.* **1992**, *98*, 5648.
[18] P. J. Stephens, F. J. Devlin, C. F. Chabalowski, M. J. Frisch, *J. Phys. Chem.* **1994**, *98*, 11623.
[19] M. J. Frisch, G. W. Trucks, H. B. Schlegel, G. E. Scuseria, M. A. Robb, J. R. Cheeseman, G. Scalmani, V. Barone, B. Mennucci, G. A. Petersson, H. Nakatsuji, M. Caricato, X. Li, H. P. Hratchian, A. F. Izmaylov, J. Bloino, G. Zheng, J. L. Sonnenberg, M. Hada, M. Ehara, K. Toyota, R. Fukuda, J. Hasegawa, M. Ishida, T. Nakajima, Y. Honda, O. Kitao, H. Nakai, T. Vreven, J. A. Montgomery, Jr, et al., *Gaussian 16, Revision C.01*, Gaussian Inc., Wallingford, CT **2016**.
[20] H. Zhang, S. Qiu, P. Tamez, G. T. Tan, Z. Aydogmus, N. V. Hung, N. M. Cuong, C. Angerhofer, D. Doel Soejarto, J. M. Pezzuto, H. H. Fong, *Pharm. Biol.* **2002**, *40*, 221.
[21] T. Tomoo, T. Nakatsuka, T. Katayama, Y. Hayashi, Y. Fujieda, M. Terakawa, K. Nagahira, *J. Med. Chem.* **2014**, *57*, 7244.
[22] C. M. Spencer, N. S. Gunasekara, C. Hills, *Drugs* **1999**, *58*, 347.
[23] Deposition Number(s) 2403816 (for 9a) contain(s) the supplementary crystallographic data for this paper. These data are provided free of charge by the joint Cambridge Crystallographic Data Centre and Fachinformationszentrum Karlsruhe Access Structures service.
[24] G. Y. J. Im, S. M. Bronner, A. E. Goetz, R. S. Paton, P. H. Y. Cheong, K. N. Houk, N. K. Garg, *J. Am. Chem. Soc.* **2010**, *132*, 17933.
[25] Y. Jiang, X. Chen, Y. Zheng, Z. Xue, C. Shu, W. Yuan, X. Zhang, *Angew. Chem. Int. Ed.* **2011**, *50*, 7304.
[26] a) J. Wang, M. Wang, K. Chen, S. Zha, C. Song, J. Zhu, *Org. Lett.* **2016**, *18*, 1178; b) Z. Long, Z. Wang, D. Zhou, D. Wan, J. You, *Org. Lett.* **2017**, *19*, 2777.

Manuscript received: March 17, 2025
Revised manuscript received: March 19, 2025
Version of record online: April 10, 2025